# Laser-generated focused ultrasound for arbitrary waveforms

Weiwei Chan,[1] Thomas Hies,[2] and Claus-Dieter Ohl[2,a)]
[1]*Interdisciplinary Graduate School, Nanyang Technological University, 50 Nanyang Avenue, Singapore 639798*
[2]*School of Physical and Mathematical Sciences, Nanyang Technological University, 21 Nanyang Avenue, Singapore 637371*

(Received 19 August 2016; accepted 29 September 2016; published online 25 October 2016)

Transducers for laser generated focused ultrasound can achieve photoacoustic waves with several hundred bars positive pressure in water. Previous designs employed concave glass substrates decorated with catalytically grown carbon nanotubes. Here, we show that arbitrarily shaped surfaces made of polymers and printed with 3d printers allow the generation of waveforms with complex temporal and spatial shape. We first present three different polymer materials together with a simplified deposition technique. This is achieved by painting layers of carbon-nanotube powder and polydimethylsiloxane. Together with a clear resin (Formlabs Photopolymer Clear Resin), pressure amplitudes of 300 bar peak positive were obtained. With the flexibility of polymer substrates, complex waveforms can be generated. This is demonstrated with a stepped surface which launches two waves separated by 0.8 $\mu$s. Detailed pressure measurements are supported with shadowgraphy images and simulations of the wave. *Published by AIP Publishing.*
[http://dx.doi.org/10.1063/1.4964852]

Baac *et al.*[1–5] demonstrated a novel focused photoacoustic source composed of a negative glass lens onto which multi-walled carbon nanotubes (MWCNT) were grown through chemical vapor deposition. The MWCNTs were embedded into a polydimethylsiloxane (PDMS) layer. The combination of a high thermal conductivity of the MWCNTs and the high thermal expansion coefficient of PDMS allows the efficient generation of photoacoustic waves which can be further amplified with a suitable focusing geometry. Baac *et al.*[1] used high numerical aperture (low f-number) lenses. In an improved version, his group recently achieved positive pressures of up to 70 MPa and sufficient negative pressures to induce cavitation in bulk water.[6] These kinds of transducers have been termed as laser generated focused ultrasound (LGFU) transducers. In all experiments discussed in this work, only green Q-switched Nd:YAG lasers with a pulse duration of about 5–6 ns are used.

In the recent years, effort was put into finding simpler approaches to manufacture yet similarly efficient absorbers of the laser light. Zou *et al.*[7] deposited gold and PDMS nanocomposite on the fiber tip to fabricate the miniature ultrasound generator. Hsieh *et al.*[8] spun a flat thin film from carbon nanofibers (CNF) and then spin-coated a PDMS film on top. They compared the pressure signals with a 30 $\mu$m thick carbon black film mixed with PDMS and found a 7.6 fold increase in the maximum pressure using the nanofibers. Chang *et al.*[9] simplified the fabrication process even further by using candle soot nanoparticles, which again were embedded in a PDMS layer. The porosity of the soot nanoparticles seems responsible for a fast heat release and the high energy-conversion efficiency of light into acoustic energy of about 0.44%. It is also possible to coat smaller glass surfaces, e.g., Colchester *et al.*[10] developed a dip coating process for fiber tips, using functionalized carbon nanotubes (C-NTs) in xylene/PDMS solution. They obtained pressures of about 4.5 MPa on a 200 $\mu$m fiber core with a laser energy of only 11.4 $\mu$J.

To generate more complex wavefronts than a single focused or planar wave, surfaces with a nontrivial shape are needed. However, the substrates of the present photoacoustic transducers are glass lenses, which limit the geometry to that offered from the lens manufacturer, e.g., planar, cylindrical, or spherical. Using arbitrarily shaped yet smooth surfaces would allow emitting photoacoustic waves with a controlled phase resembling hologram. The added manufacturing aka 3d-printing technology promises to construct polymer based surfaces with high accuracy at low cost.[11,12] These surfaces need to be sufficiently transparent to light, smooth, and offer good acoustic properties. Additionally, we need to develop a deposition technique compatible with the low melting temperature of the transducer substrates.

In this work, we demonstrate three 3d-printing techniques for LGFU transducers, and one of them reveals similar if not a better performance than a glass substrate. In particular, we discuss the fabrication of the transducer substrate and coating with a PDMS-CNT paint. Then we measure the acoustic waves temporally and spatially resolved before we present a complex waveform generated from a stepped surface using shadowgraphy imaging and compare the results with simulations.

The substrates supporting the photoacoustic layer are 3d-printed with three different kinds of printers: a stereolithography printer (Form 1+, Formlabs, Sommerville, MA, USA), a high-resolution jet printer (Objet Eden260VS, Stratasys, Eden Prairie, MN, USA), and a filament printer (Ultimaker 2, Geldermalsen, the Netherlands). Materials with high transparency at the laser wavelength of 532 nm are available for stereolithography and ink-based printers;

a)Electronic mail: cdohl@ntu.edu.sg

filament printers need a second molding step to obtain a transparent substrate.

Photoacoustic waves may have frequency components of 10 MHz and above which relates to a wavelength of 150 $\mu$m, setting the scale of the necessary surface roughness to control the phase. In particular for the filament printer, after printing the negative of the envisioned shape with a 400 $\mu$m diameter nozzle, we smoothened the surface by dissolving the polylactide filament mildly with acetone. This printed part served as a mold for casting the substrate out of the transparent heat curing rubber material PDMS (Sylgard 184, polymer to current agent ratio 10:1). In contrast, the jet based and the stereolithography printer can be directly printed as a transparent substrate, thus the molding step is omitted and the absorption layer is applied directly on the printed material.

Therefore, the surface of the substrate was cleaned with ethanol and deionized water and dry blown with nitrogen. Then in total, 5 layers were deposited starting with a layer of carbon nanotube powder (MWCNT powder, ceEntek Pte Ltd., Singapore), followed by a thin layer of PDMS, and then again MWCNT powder, and a second thin layer of PDMS. The topmost layer is an approximately 100 nm thick layer of gold. Both PDMS layers were deposited by spin coating at 2000 rpm for 1 min and cured at 80 °C for 1 h. The CNT powder was deposited by simply brushing it onto with a clean cotton brush. After curing the last PDMS layer, a gold layer was deposited through sputtering for 60 s at 10 mA current. This last step increases the optical extinction of the photoacoustic layer 1. The performance of the 3d-printer transducers is compared to a LGFU transducer made of a glass substrate (Thorlabs, N-BK 7 glass) while following the same coating process.

The substrate of the transducers is designed using the constructive solid geometry software OpenScad (http://www.openscad.org). Here, we limit the study to two designs. The first is a concave spherical cap with a radius of curvature of 10 mm and an opening diameter of 15 mm resulting into a f-number of f/0.67, see Figs. 1(a) and 1(b). The small f-number predicts a pressure gain of $G \approx 200$ at the acoustic focus for frequencies of 15 MHz, see Baac *et al.*[1] The second design contains besides the same spherical surface a 1.2 mm lowered circular plane surface with a diameter of 4.0 mm, see Figs. 1(c) and 1(d). The design goal of this stepped surface was to generate two waves with temporal spacing, here of 0.8 $\mu$s.

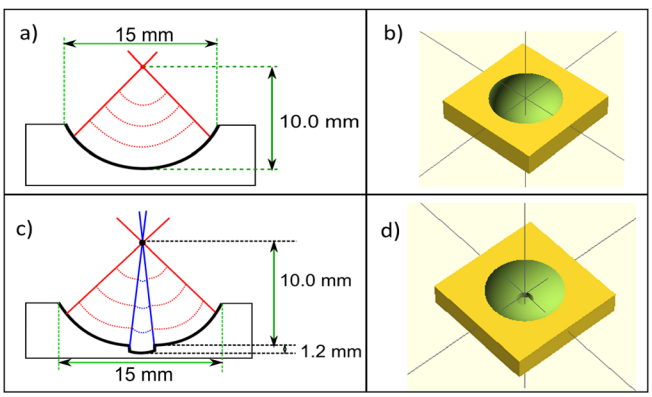


FIG. 1. (a) Side view and (b) 3d sketch of the substrate for single wave excitation. The radius of curvature is 10 mm and the opening aperture is 15 mm in diameter. (c) Side view and (d) 3d sketch of the stepped substrate. The 4.0 mm diameter, planar circular step is 1.2 mm below the spherical surface.

In the supplementary material, Figure 1 shows the experimental setup to measure the performance of the 3d-printed LGFU transducers and visualize the acoustic waves in the liquid. The photoacoustic source was placed on the bottom of an acrylic tank filled with deionized water. A Q-switched laser (Litron Nano Series, Nano L 34010, Q-switch, Nd:YAG laser, $\lambda = 532$ nm, pulse width 5 ns) generates the photoacoustic waves. The beam with approximate 10 mJ/cm$^2$ is first expanded to a diameter of 10 mm and is reflected off from a mirror onto the source. A second short pulsed laser visualizes the waves through a collimated illumination beam (NewWave Orion, Nd:YAG laser, $\lambda = 532$ nm, pulse width 6 ns). The illumination laser pumps a fluorescent dye cell (Exciton, LDS 698, Dayton, OH, USA), which reduces speckles and separates the excitation light from the illumination ($\lambda = 698$ nm). The red emission is collected with a glass fiber (not shown in the figure) and brought to the scene through collimation optics. The firing of the two lasers is synchronized with a digital delay generator (BNC 575, Berkley Nucleonics Corporation, San Rafael, CA, USA). A sensitive camera (Andor Zyla 5.5, Belfast, Northern Ireland) with a 10× microscope objective (Mitutoyo plan apo infinity corrected long working distance objective, 33.5 mm) images shadowgraphs of the wave fronts. The pressure waves are measured with a glass fiber hydrophone (HFO-690, Onda, Sunnyvale, CA, USA). The frequency response of the hydrophone is specified between 3 kHz to 150 MHz with a typical sensitivity of about 6 mV/MPa. The signal is recorded with a digital storage oscilloscope (Waverunner 64xi, Teledyne LeCroy, Chestnut Ridge, NY, USA).

The simulations of the pressure field are done with a finite element solver for the linear wave equation (COMSOL 5.2, COMSOL, Inc., Burlington, MA, USA). We implement the geometry and use appropriate boundary conditions: the pressure on the surface of the transducers is given as a function of space and time. For simplicity, we assume a single cycle sinusoidal wave which is achieved through Gaussian enveloped harmonic function

$$p_{ex}(t) = -\exp\left[-\frac{(t-t_0)^2}{2d^2}\right]\sin\left[2\pi f(t-t_0)^2\right], \qquad (1)$$

where the full width at half maximum (FWHM) of the envelope is approx. $2.35d = 32$ ns and $f = 10$ MHz, the fundamental frequency of the photoacoustic wave. Here, the dependent variable is the pressure along the travelling direction. Accounting for the spherical shape of the surface and assuming a top flat illumination light, the pressure on the surface is

$$p(x,t) = p_{ex}(t)\sqrt{1-\left(\frac{r}{R}\right)^2}. \qquad (2)$$

For the stepped transducer, the lower part is modelled as a plane wave, i.e., omitting the square root in Eq. (2). We implement the plane wave radiation conditions to mitigate

reflections at the liquid boundaries and the glass fiber hydrophone is modelled as a hard reflector. For more details, see the supplementary material.

We first characterize the effect of the material emitted peak positive pressure while keeping the laser energy constant. Only the spherical surfaces are tested, i.e., the ones shown in Figs. 1(a) and 1(b). The substrate material is varied between glass, VeroClear (RGD 810, Stratasys, Eden Prairie, MN, USA), Clear Resin (Clear, FLGPLC02, Formlabs, Somerville, MA, USA), and PDMS. Care was taken that similar coating thicknesses were applied for each of the samples. First the position of the maximum pressure was determined by stepping through the acoustic field. Then the pressure signal as a function of the laser energy was measured. For each point, 10 measurements were conducted and an average value with the standard deviation as error bars is plotted in Fig. 2. We see that the resin and glass show a similar response with laser fluence, while VeroClear and PDMS achieved about 30% and 45% lower pressures.

Likely the response of the different substrate materials is connected to the acoustic properties of the substrate. For example a material perfectly matched with the acoustic impedance of water would radiate only half the acoustic energy in the forward direction. Yet shear waves in the solid and interfacial waves between the solid and the liquid reduce the available energy further. Some mechanical and optical properties of the 4 substrate materials are provided in the supplementary material. The maximum positive pressure amplitudes we could achieve were 290 bar for the glass substrate and 300 bar for the resin when the laser was operated at 20 mJ/cm$^2$. The film of mixture did not show deterioration of the pressure signal for 10 successive shots and the pressure signal was stable.

Next we characterize the focusing of the positive and negative pressure. Figure 3 summarizes the pressure measurements along the axial (z-axis) direction, see the supplementary material, Figure.1. The error bars are the standard deviation from 10 measurements. The laser input energy was kept constant at approximately $10 \pm 0.15$ mJ/cm$^2$. Glass and resin show very similar behavior for the positive amplitude. The pressure rises within 1 mm from 30 bar to 110 bar and drops over a similar distance, yet the negative pressures

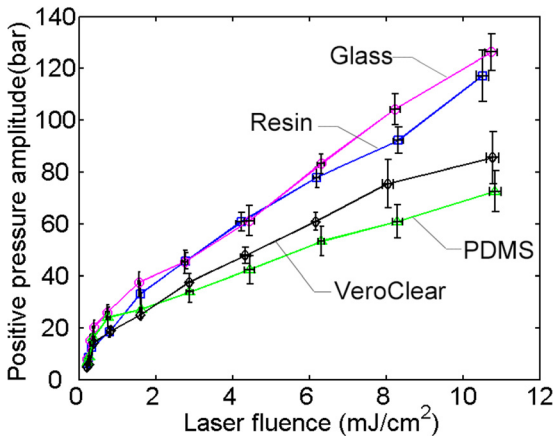


FIG. 2. Measured peak pressure amplitude for the four different substrate materials as a function of the laser fluence.

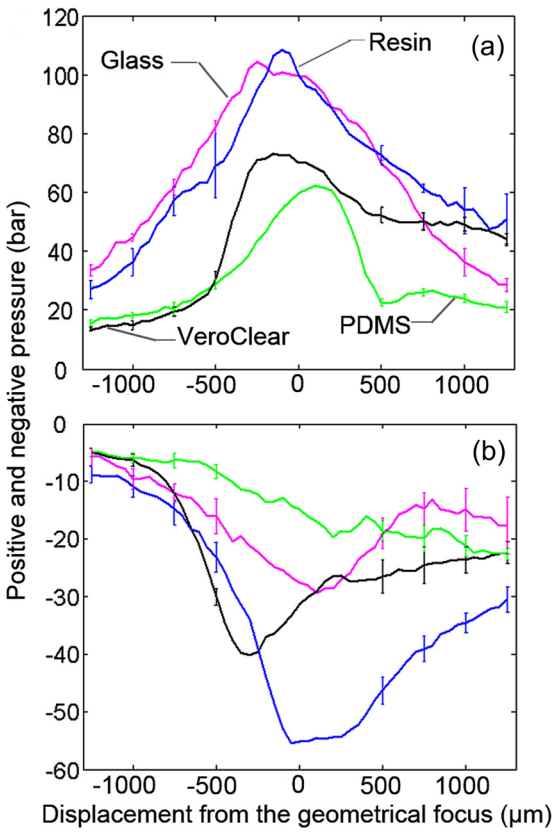


FIG. 3. The pressure distribution near the focal point of the simple spherical transmitter of four different materials (laser energy at the transmitter bottom ~10 mJ/cm$^2$). (a) Depicts the positive amplitude while (b) the negative amplitude.

achieved differ greatly, with about 3 times lower pressures for the resin. While the axial pressure distribution has a length scale of 1–2 mm, the radial pressure distribution is considerably narrower. Figure 4 compares the pressure distribution of resin (left) with the glass substrate (right). Although there is some asymmetry we find an approximate full width at half maximum (FWHM) of the peak pressure of 250 $\mu$m for resin, and 400 $\mu$m for the glass substrate.

Pressure recordings at the focus are shown in Fig. 5(a). Time $t = 0$ is the moment the laser pulse is launching the pressure wave. Assuming a speed of sound of $c = 1481$ m/s at 20 °C we expect the wave to reach at $t = 6.75$ $\mu$s focus and about 30 ns after the expected time, or a spatial offset of 44 $\mu$m. This distance is less than half the diameter of the glass fiber hydrophone and may be caused by manufacturing uncertainty or the limited resolution of the spatial scanning.

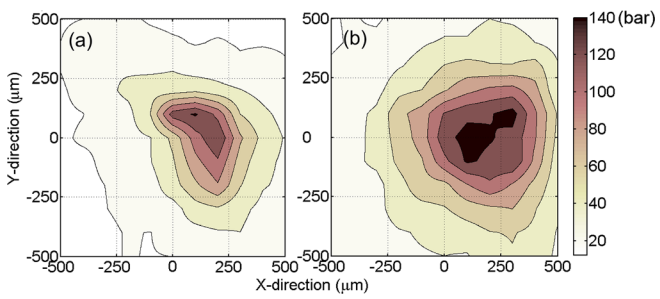


FIG. 4. Positive pressure distribution from the resin (a) and the glass (b) substrate.

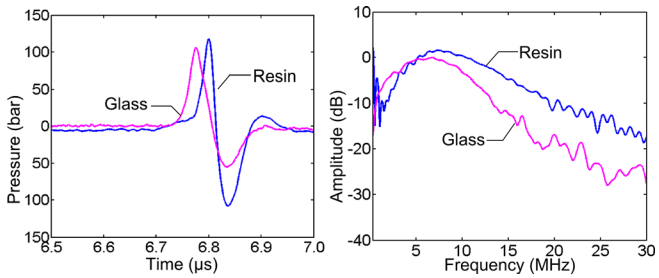


FIG. 5. (a) The pressure measurement at the focus; (b) the frequency spectra from the glass and the resin substrates, normalized to the maximum amplitude of the glass substrate.

Interestingly, the signal from the resin shows a considerably faster rise time and the positive pulse is followed by a larger negative tail as compared to the glass substrate. This is also evident in the spectrum of both waves shown in Fig. 5(b). Both spectra were normalized to the maximum amplitude of the glass substrate, i.e., the maximum amplitude of the glass substrate is taken as the reference pressure when calculating the frequency spectra. There, the maximum frequency of the glass is about 6.7 MHz, while the resin shows about 8.3 MHz. Baac *et al.*[1] found about twice the frequencies from their vapor deposited CNTs. The better control of the active emitter thickness through their deposition technique but also their fiber hydrophone having a smaller light sensitivity, may contribute to this difference. Yet the advantage of a greatly simplified protocol of brushing CNTs and spin coating PDMS allows achieving results of similar range and with the added flexibilities.

We now study the stepped transducer design as shown in Figs. 1(c) and 1(d). Figure 6(a) displays the selected frames

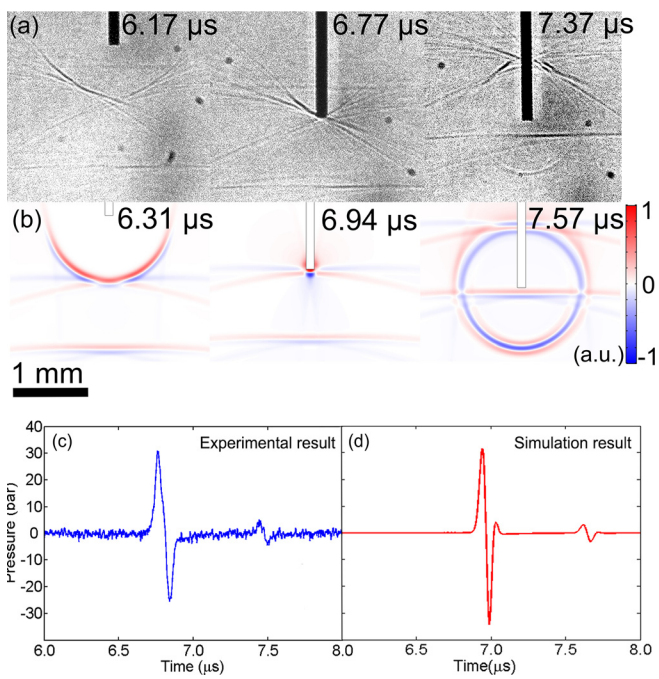


FIG. 6. Experimental simulations of the stepped transducer. (a) Shadowgraphs of the waves approaching the hydrophone tip (please note that only the camera is moved, the hydrophone remains at the focus). (b) Simulation of the pressure field using a linear wave propagation model. (c) Measured pressure at the focus and (d) simulated pressure at the focus.

of the wave propagation taken with the shadowgraphy setup. To obtain the pictures at the indicated times, we delay the pulsed illumination with respect to the laser pulse generating the photoacoustic wave. This allows recording the wave propagation without motion blurring. The field of view of Fig. 6(a) is approximately $3 \times 3\,\text{mm}^2$. The black vertical strip is the hydrophone whose tip is aligned with the pressure focus. Only the camera position is adjusted between $t = 6.17\,\mu$s and $6.77\,\mu$s in Fig. 6(a). The time $t = 0$ coincides with wave generated on the LGFU surface. At time $t = 6.77\,\mu$s, the primary wave is focused onto the tip of the glass fiber, while at $t = 7.37\,\mu$s, the second wave travels closer to the fiber tip. Please note that a spherical wave is emitted from the glass fiber as a result of the reflection of the primary wave. We find that at sufficient high pressures, cavitation is generated on the glass fiber tip, which is the result of diffraction waves starting at the circular rim of the fiber.[13,14] As these waves overlap on the axial center of the fiber, sufficient tension is reached to form a cavity on the glass surface. This is also clearly evident from the hydrophone signal because the fiber hydrophone measures the change of the index of refraction of water. While we see cavitation on the fiber tip we have not observed cavitation in the free field under all operation conditions of the tested transducers.

The simulated pressure field is shown in Fig. 6(b) using red color for positive pressures and blue for negative. For details on the simulation method, see the supplementary material. At $t = 6.31\,\mu$s, the spherical focused wave entering the field of view is trailed by a planar wave from the lens step by $0.8\,\mu$s. The spherical wave is focused precisely on the tip of the hydrophone resulting into a reflected spherical wave. From Fig. 6(a), the shadowgraphy image shows a nice agreement with the simulated pressure field in Fig. 6(b), including the first spherical wave, the second planar wave, and the reflective wave from the fiber tip. We can conclude that the linear wave model is sufficient to capture the overall wave dynamics, and finite amplitude effects are relevant for the unresolved last stage of focusing. This allows using the toolset such as diffraction integrals and back-propagation of linear waves to design suitable surfaces for the desired pressure distribution.

See supplementary material for Figure 1.

In this work laser-generated focused ultrasound (LGFU) from arbitrarily shaped surfaces has been demonstrated where the surfaces are made through 3d-printing. The low melting point of the surface made it necessary to develop a compatible coating process. We found that the LGFU transducer made of resin using a stereolithography printer achieved the highest efficiency and gave comparable results with that from a glass substrate. We speculate that the findings offer interesting solutions for LGFU transducer design. In particular for the generation of minimum diffraction Bessel beams, compact Fresnel lenses, miniaturized lenses for lab-on-a-chip application, and multifoci and sequences of shock waves. At the current state we find that simulations using a linear acoustic wave model capture the wave propagation well. Yet, modeling the pressure generation with our coatings has not been done. Here, an approach following Tong *et al.*[15] may be used.

[1]H. W. Baac, J. G. Ok, A. Maxwell, K.-T. Lee, Y.-C. Chen, A. J. Hart, Z. Xu, E. Yoon, and L. J. Guo, "Carbon-nanotube optoacoustic lens for focused ultrasound generation and high-precision targeted therapy," Sci. Rep. **2**, 989 (2012).
[2]H. W. Baac, J. Frampton, J. G. Ok, S. Takayama, and L. J. Guo, "Localized micro-scale disruption of cells using laser-generated focused ultrasound," J. Biophotonics **6**, 905–910 (2013).
[3]H. W. Baac, T. Lee, J. G. Ok, T. Hall, and L. J. Guo, "Dual-frequency focused ultrasound using optoacoustic and piezoelectric transmitters for single-pulsed free-field cavitation in water," Appl. Phys Lett. **103**, 234103 (2013).
[4]H. W. Baac, J. G. Ok, T. Lee, and L. J. Guo, "Nano-structural characteristics of carbon nanotube-polymer composite films for high-amplitude optoacoustic generation," Nanoscale **7**, 14460–14468 (2015).
[5]H. W. Baac, T. Lee, and L. J. Guo, "Micro-ultrasonic cleaving of cell clusters by laser-generated focused ultrasound and its mechanisms," Biomed. Opt. Express **4**, 1442–1450 (2013).
[6]T. Lee, J. G. Ok, L. J. Guo, and H. W. Baac, "Low f-number photoacoustic lens for tight ultrasonic focusing and free-field micro-cavitation in water," Appl. Phys. Lett. **108**, 104102 (2016).
[7]X. Zou, N. wu, Y. Tian, and X. Wang, "Broadband miniature fiber optic ultrasound generator," Opt. Express **22**, 18119–18127 (2014).
[8]B.-Y. Hsieh, J. Kim, J. Zhu, S. Li, X. Zhang, and X. Jiang, "A laser ultrasound transducer using carbon nanofibers-polydimethylsiloxane composite thin film," Appl. Phys. Lett **106**, 021902 (2015).
[9]W.-Y. Chang, W. Huang, J. Kim, S. Li, and X. Jiang, "Candle soot nanoparticles-polydimethylsiloxane composites for laser ultrasound transducers," Appl. Phys. Lett **107**, 161903 (2015).
[10]R. J. Colchester, C. A. Mosse, D. S. Bhachu, J. C. Bear, C. J. Carmalt, I. P. Parkin, B. E. Treeby, I. Papakonstantinou, and A. E. Desjardins, "Laser-generated ultrasound with optical fibres using functionalised carbon nanotube composite coatings," Appl. Phys. Lett **104**, 173502 (2014).
[11]J. Micallef, *Beginning Design for 3D Printing* (Apress, 2015).
[12]L. Jonušauskas, E. Skliutas, S. Butkus, and M. Malinauskas, "Custom on demand 3d printing of functional microstructures," Lith. J. Phys. **55**(3), 227–236 (2015).
[13]M. Frenz, G. Paltauf, and H. Schmidt-Kloiber, "Laser-generated cavitation in absorbing liquid induced by acoustic diffraction," Phys. Rev. Lett. **76**, 3546 (1996).
[14]M. Mohammadzadeh, S. R. Gonzalez-Avila, Y. C. Wan, X. Wang, H. Zheng, and C.-D. Ohl, "Photoacoustic shock wave emission and cavitation from structured optical fiber tips," Appl. Phys. Lett. **108**, 024101 (2016).
[15]L. Tong, C. Lim, and Y. Li, "Generation of high-intensity focused ultrasound by carbon nanotube opto-acoustic lens," J. Appl. Mech. **81**, 081014 (2014).